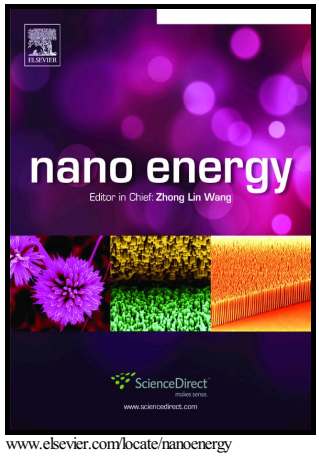

www.elsevier.com/locate/nanoenergy

Highly acid-durable carbon coated Co_3O_4 nanoarrays as efficient oxygen evolution electrocatalysts

Xiulin Yang, Henan Li, Ang-Yu Lu, Shixiong Min, Zacharie Idriss, Mohamed Nejib Hedhili, Kuo-Wei Huang, Hicham Idriss, Lain-Jong. Li

PII: S2211-2855(16)30089-1
DOI: http://dx.doi.org/10.1016/j.nanoen.2016.04.035
Reference: NANOEN1240

To appear in: *Nano Energy*

Received date: 24 February 2016
Revised date: 7 April 2016
Accepted date: 19 April 2016

Cite this article as: Xiulin Yang, Henan Li, Ang-Yu Lu, Shixiong Min, Zacharie Idriss, Mohamed Nejib Hedhili, Kuo-Wei Huang, Hicham Idriss and Lain-Jong Li, Highly acid-durable carbon coated Co_3O_4 nanoarrays as efficient oxygen evolution electrocatalysts, *Nano Energy* http://dx.doi.org/10.1016/j.nanoen.2016.04.035

Highly acid-durable carbon coated Co_3O_4 nanoarrays as efficient oxygen evolution electrocatalysts

Xiulin Yang[a], Henan Li[a], Ang-Yu Lu[a], Shixiong Min[b], Zacharie Idriss[c], Mohamed Nejib Hedhili[a], Kuo-Wei Huang[b], Hicham Idriss[c], Lain-Jong Li[a*]

[a]*Physical Science and Engineering Division, King Abdullah University of Science & Technology (KAUST), Thuwal 23955-6900, Saudi Arabia.*

[b]*KAUST Catalysis Center, King Abdullah University of Science and Technology, Thuwal 23955-6900, Kingdom of Saudi Arabia*

[c]*SABIC, Corporate Research and Innovation (KAUST), Saudi Arabia*

*To whom correspondence should be addressed: lance.li@kaust.edu.sa

Abstract

Most oxygen evolution reaction (OER) electrocatalysts are not stable in corrosive acids. Even the expensive RuO_2 or IrO_2, the most acid-resistant oxides, can be dissolved at an oxidative potential. Herein, we realize that the failures of OER catalysts are mostly caused by the weak interface between catalysts and the substrates. Hence, the study of the interface structure between catalysts and substrates is critical. In this work, we observe that the cheap OER catalysts Co_3O_4 can be more durable than the state-of-the-art RuO_2 if the interface quality is good enough. The Co_3O_4 nanosheets deposited on carbon paper (Co_3O_4/CP) is prepared by electroplating of Co-species and followed by a two-step calcination process. The 1st step occurs in vacuum in order to maintain the surface integrity of the carbon paper and converts Co-species to Co(II)O. The 2nd step is a calcination in ambient conditions which enables the complete transformation of Co(II)O to Co_3O_4 without degrading the mechanical strength of the Co_3O_4-CP interface. Equally important, an in situ formation of a layer of amorphous carbon on top of Co_3O_4 further enhances the OER catalyst stability. Therefore, these key advances make the Co_3O_4 catalyst highly active toward the OER in 0.5 M H_2SO_4 with a small overpotential (370 mV), to reach 10 mA/cm^2. The

observed long lifetime for 86.8 h at a constant current density of 100 mA/cm^2, is among the best of the reported in literature so far, even longer than the state-of-art RuO_2 on CP. Overall, our study provides a new insight and methodology for the construction of a high-performance and high stability OER electrocatalysts in corrosive acidic environments.

Keywords: Oxygen evolution reaction; carbon coated Co_3O_4; Electrolysis; Catalysis

Introduction

Hydrogen is a clean energy carrier poised to provide civilizations with the needed alternatives to curb CO_2 emission. Water splitting by electrolyzers is a promising method to produce hydrogen in a large scale [1-7]. The efficiency and price-performance ratio of hydrogen evolution reaction (HER) at cathodes has considerably improved upon the use of non-expensive catalysts such as MoS_x, FeP and CoP [8-17]. Hydrogen production with water splitting is therefore mainly limited by the kinetics of oxygen evolution reaction (OER) at the anodes [18, 19]. The best electrocatalysts for OER so far are the metal or oxide forms of Ir, Ru, and their alloys. However, their scarce nature and associated high-cost considerably limit large-scale implementation to industrial devices. Over the past few years, great efforts have been devoted to exploring cheap and efficient OER catalysts based on earth abundant elements, such as Co, Fe, Ni and Mn oxides/hydroxides [20-24], phosphides [25-27], dichalcogenides and some non-metallic compounds [28-30], as alternative OER catalysts in an alkaline solution. However, the development of alkaline water electrolysis is restricted by several issues including low current density and cross-diffusion of the produced gases [31]. By contrast, the proton exchange membrane (PEM) electrolysis in acids has shown critical advantages in current densities, voltage efficiency and purity of produced gases. Thereafter, several anode catalysts likely suitable in acids have been reported, such as RuO_2, IrO_2, and their ternary oxides [32-34]. To reduce the

usage of Ru and Ir, several other metal elements including Sn, Sb, Nb, Pb, Ni, Cu, Ta, Zr and Mo, have been added to form alloys or core-shell structures [35-40].

The OER involves complex pathways of high activation energy and energetic intermediates. Taking IrO_2 as one example, the adsorbed OH-group will be oxidized to several oxygenated species accompanied with the transformation of iridium cations to different oxidation states. Corrosion on IrO_2 will take place in parallel with O_2 evolution ($IrO_3 + H_2O \rightarrow IrO_4^{2-} + 2H^+$) [41]. Similarly, RuO_2 also suffers from substantial corrosion during O_2 evolution in acid electrolytes at high current densities [42]. Recently, the spinel Co_3O_4 has attracted attention for OER owing to its low cost, excellent catalytic properties, and high corrosion stability in alkaline solutions [43, 44]. However, the application of Co_3O_4 for OER in acids is almost stagnant because the spinel Co_3O_4 also suffers from anodic corrosion at potentials higher than 1.47 V (*vs.* RHE) [45], in which the formed CoO_2 decomposes into soluble CoO with the simultaneous liberation of the O_2 [46]. In addition to dissolution mechanism, it is actually found that the failure of most OER electrodes originates from the degradation of the substrates as well as the poor adhesion between Co_3O_4 and this substrate. Hence, the selection of substrate is very critical. For example, Ti is a typically used substrate for OER. The adhesion between a Ti foil and Co_3O_4 is weak and the Co_3O_4 is easily delaminated from the Ti foil substrate [47, 48]. This was also observed in the case of the OER system composed of IrO_2/Ti interface [49]. Carbon paper-based electrode is an alternative option for the electrode substrate due to their large surface area, good electric conductivity, and excellent chemical stability in a wide variety of liquid electrolytes [50, 51]. We have compared two carbon electrodes, carbon cloth (CC) and carbon paper (CP) with various treatments, and found that the CP exhibits much better stability and presents better adhesion to our Co_3O_4 catalysts during OER (see supporting **Figure S1a and S1b**). Note that in our

experiment the only difference of the two catalysts is the substrates. Hence, it can be ascribed that more sp^2 carbon (as in the case of CP) in the skeleton can greatly improve the OER stability (see **supporting Figure S1c**). This is also consistent with the widely accepted observation that graphene (sp^2-carbon) based 6-member ring is more oxidation- and acid-resistant than the amorphous sp^3 carbons. Thus, CP is applied as the substrate for OER reaction in caustic acids or alkali conditions for all the experiments presented in this manuscript.

To obtain the target catalytic material Co_3O_4 with strong bonding to CP, we have electroplated the Co-species on CP followed by thermal oxidation to synthesize Co_3O_4 nanosheets. It was observed that the post-oxidation process critically affected the stability the Co_3O_4-carbon paper interface and thus the OER stability. Here we have successfully developed a two-step calcination process, where the 1st step is in vacuum which reinforces the surface integrity of the carbon paper and converts Co-species to CoO and the 2nd step is calcination in ambient conditions enabling the complete transformation to Co_3O_4. Moreover, a layer of amorphous carbon coating on Co_3O_4 could effectively avoid the catalyst peeling off from carbon substrates and further extend the long-time OER stability. The optimized protocol of amorphous carbon coated by Co_3O_4 (Co_3O_4@C) provided low over-potentials of 370 mV and 310 mV to achieve the current density of 10 mA/cm^2 in acid and alkaline conditions, respectively. Furthermore, the stability tests show that the OER electrode was stable up to 86.8 h and 413.8 h (at 100 mA/cm^2) in acid and alkaline conditions, respectively. The electrode breakdown time is so far the longest compared with available literature, which suggests that the prepared Co_3O_4-based catalyst is a promising non-precious-metal catalyst for OER.

Experimental Section

Materials:

All chemical reagents including cobalt(II) nitrate hexahydrate, glucose, potassium hydroxide (KOH), sulfuric acid (H_2SO_4) and ethanol were purchased from Sigma Aldrich. Millipore water from a Millipore Q water purification system was used in all experiments.

Electrochemical deposition of Co-species on carbon fiber paper: The carbon paper (CP) with the size 1 cm × 2.5 cm was first soaked with ethanol, and then oxidized in 0.5 M H_2SO_4 solution with cyclic voltammetry for 10 cycles between 1.5 to 2.3 V (vs. Ag/AgCl, in saturation KCl solution). The part of oxidized CP (1 cm × 1 cm) was then immersed into a 0.1 M $Co(NO_3)_2$ solution for the electrodeposition of Co-species. A Pt foil and an Ag/AgCl (in saturation KCl solution) electrode were used as the counter and reference electrodes respectively. Electrodeposition was performed at a constant current mode (-10 mA/cm^2) from 10 to 60 min in a PGSTAT 302N Autolab workstation. The as-deposited sample was then exposed to air to form oxide and hydroxide surface layers for further treatment (Co-species/CP).

Preparation of Carbon coated Co_3O_4 on CP:

The prepared Co-species/CP was immersed into 5 mg/mL glucose solution for 4 h under slow agitation condition, and then taken out and dried at room temperature. The glucose coated Co-species/CP was put into a tube furnace and then pumped under vacuum (<5 mTorr). The furnace was then heated to 350 ^oC in 2 h and kept at this temperature for another 1 h. After that, the vacuum pressure was adjusted to 1000 mTorr by passing air into the furnace chamber and kept for 4 h, where the glucose was thermally decomposed to amorphous carbon and uniformly covered on the formed Co_3O_4/CP [Co_3O_4@C/CP(vacuum 1h + air 4h)]. For comparison, Co_3O_4/CP without carbon modification (vacuum 1h + air 4h) was prepared at the same experiment conditions indicated above. The CoO/CP (vacuum 1h) was prepared via only vacuum treatment, and the Co_3O_4/CP (air 5h) was also prepared by heating in air at 350 °C for 5 h. The

Co_3O_4 catalyst loading amount on CP (50 min) was determined to be 12.6 mg using a high precision weighing balance.

Preparation of nafion coated Co_3O_4/CP and RuO_2/CP:

The Co_3O_4 and RuO_2 powder were prepared by directly annealing $Co(NO_3)_2 \cdot 6H_2O$ and $RuCl_3$ precursors in a porcelain boat and placed in a muffle furnace, and then heated to 350 ^oC with a ramp of 2.5 ^oC/min and maintained for 5 h in air. After that, the furnace was allowed to cool to room temperature.

As for the synthesis of Co_3O_4@nafion/CP catalyst, 62.5 mg Co_3O_4 powder was first dispersed in a mixed solvent consisting of 0.5 mL of 2-propanol and 0.5 mL of water, and the mixture was ultrasonicated for 30 min by using ultrasonic oscillators. Then, 200 μL of the well-dispersed mixture was drop-coated on the acid-oxidized CP, and 70 μL of 1.0 wt.% Nafion solution in 2-propanol was added to fix the catalyst onto the CP surface, and further dried at 40 ^oC in air for electrochemical measurements. In addition, RuO_2 on acid-oxidized CP (RuO_2@nafion/CP) was prepared using similar procedures as described above.

Reference electrode calibration:

The electrochemical measurements were performed in a PGSTAT 302N Autolab Potentiostat/Galvanostat (Metrohm). A graphite rod and an Ag/AgCl (in saturation KCl solution) electrodes were used as the counter and reference electrodes respectively. The solutions used for reference electrode calibration were 0.5 M H_2SO_4 and 1.0 M KOH solutions purged with H_2 for 30 min prior to measurements. The reference electrode calibration was performed in a high purity hydrogen saturated electrolyte solution with a Pt wire as the working and counter electrodes, respectively. The current-voltage curves were scanned at a scan rate of 5 mV/s, and

the average of the two potentials at which the current crossed zero was taken to be the thermodynamic potential for the hydrogen electrode reactions (See **Figure S2** for details). Our result shows that the E(Ag/AgCl) is lower than E(RHE) by 0.217 V in 0.5 M H_2SO_4 and by 1.014 V in 1 M KOH.

Electrochemical measurements:

The OER activity of Co_3O_4@C/CP was evaluated by measuring polarization curves with linear sweep voltammetry (LSV) at a scan rate of 5 mV/s in 0.5 M H_2SO_4 and 1.0 M KOH solutions. The stability test for the Co_3O_4@C/CP catalysts was performed with the time dependent potential measurement, where a constant current density (100 mA/cm^2) was provided. All data have been corrected for a small ohmic drop based on impedance spectroscopy.

Characterization:

The field-emission scanning electron microscope (FESEM, FEI Quanta 600) was used to observe the surface morphology of the catalysts and electron energy loss spectroscopy (EELS) mapping. The nanoscale crystal structure was revealed by a transmission electron microscopy (FEI Titan ST, operated at 300 KV). The crystalline structure of the samples was analyzed by X-ray diffraction (XRD, Bruker D8 Discover diffractometer, using Cu Kα radiation, λ = 1.540598 Å). Raman spectrometer LabRAMAramis (HoribaJobinYvon) was employed and the range of 100-3500 cm^{-1} was explored. A Diode-pumped solid-state (DPSS) laser with wavelength of 473 nm was used as the excitation source. The laser power on the sample surface was adjusted using different filters to avoid the heating effects on the sample. Fourier transform infrared spectroscopy (Nicolet iS10 FT-IR spectrometer, Thermo Scientific) was used to characterize the functionalized groups and catalysts on carbon fibers. XPS studies were carried out in a Kratos

Axis Ultra DLD spectrometer equipped with a monochomatic Al Kα x-ray source (hν = 1486.6 eV) operating at 150 W, a multichannel plate and delay line detector under a vacuum of 1×10−9 mbar. The survey and high-resolution spectra were collected at fixed analyzer pass energies of 160 eV and 20 eV, respectively. Binding energies were referenced to the C 1s peak (set at 284.4 eV) of the sp2 hybridized (C=C) carbon from the sample.

Results and discussion

Preparation and crystal structure of Co_3O_4-based OER

As schematically illustrated in **Figure 1a**, the Co-species were electrodeposited onto a carbon paper in a standard three-electrode system, where the 0.1 M $Co(NO_3)_2$ solution was used and the current density was kept at -10 mA/cm^2. The electrodeposited Co-species were left in air over night before the calcination was performed. It is important to mention that Co-species cannot be directly deposited on a CP without surface treatment because the pristine CP is hydrophobic. For better adhesion between Co-catalysts and the CP substrates, hydrophilic treatment with an acid was found to be necessary. Hence, all the CP substrates used in this work were prior treated with acids unless specified otherwise. The XRD pattern in **Figure S3** for the electrodeposited Co-species on CP (Co-species/CP) indicates that it is a mixture of $Co(OH)_2$, CoO and disordered Co_3O_4.

In oxygen-deficient annealing conditions (one hour at 350 ^oC in vacuum; ~5 mTorr), the Co-species is mainly converted to CoO (sample abbreviated as CoO/CP). By contrast, post treatment at 350 ^oC in air leads to the formation of Co_3O_4 (sample abbreviated as Co_3O_4/CP). The carbon-coated Co_3O_4 was prepared by immersing the Co-species/CP in a 5 mg/mL glucose solution for about 4 h, followed by the two-step post treatment at 350 ^oC, in vacuum for 1 h and then in air for 4 h (sample abbreviated as Co_3O_4@C/CP). We observe that the thickness of the carbon

coating depends on the glucose concentration. Supporting **Figure S4** shows that the 5 mg/L is the optimized glucose concentration for our Co_3O_4 catalysts in terms of the lifetime extention for OER. Since the glucose (after high temperature annealing) is used as a binding material to secure the catalysts on CP, its capability to prevent the catalyst from peeling initially increases with the glucose concentration. However, when the binding layer becomes too thick, its mechanical property may become dominant. Hence the stability of OER catalysts starts to decrease with the glucose concentration. The crystal structures of the obtained CoO/CP, Co_3O_4/CP and Co_3O_4@C/CP were confirmed by the XRD analysis in **Figure 1b**. The broad peaks at $2\theta = 26.2^{\circ}$ and 53.9° are associated with the (002) and (004) planes of the graphite-like structure of the CP. The other peaks for the sample after 1 h vacuum (5 mTorr) treatment can be attributed to the cubic structure of CoO (JCPDS no. 65-2902), and the XRD peaks for the sample treated in air 5 h and the carbon-coated sample after two-steps treatment are similar, which are ascribed to the cubic structure of the Co_3O_4 (JCPDS no. 42-1467). The electrodeposited Co-species/CP are further characterized by scanning electron microscopy (SEM) as shown in **Figure 1c**, where the CP surface is fully covered with randomly oriented nanosheets. These high surface area nanosheet structures still maintain their morphologies after glucose-soaked Co-species is fully converted into carbon-layer coated Co_3O_4 as shown in **Figure 1d**. It can be explained as that with the arising heating temperature in oxygen-deficient condition, the adsorbed glucose molecules start to dehydrates and cross-links, and as the reaction continues, aromatization and carbonization will further take place, resulting in formation carbonized shell covering on the surfaces of Co_3O_4 sheet-like structures [52].

Transmission electron microscopy (TEM) and high-resolution TEM (HRTEM) were used to reveal the structures of flakes that were peeled off from the Co_3O_4@C/CP electrode. A layer of

amorphous carbon with the thickness of ~ 3.6±0.5 nm is found to be uniformly coated on the Co_3O_4 crystals as shown in **Figure 2a**. The HRTEM images for the selected area and the corresponding electron diffraction (FFT – Fast Fourier Transform) pattern in **Figure 2b** show two lattice spacings of 0.28 and 0.23 nm, corresponding to the Co_3O_4 crystal planes (220) and (222), respectively. The crystal was further analyzed by their selected area electron diffraction (SAED) patterns as shown in supporting **Figure S5**, in which several intense spots in random orientation assigned to the cubic crystalline structures. Furthermore, the Co_3O_4@C nanocomposite was analyzed by high-angle annular diffraction field scanning transmission electron microscopy (HAADF-STEM) as shown in **Figure 2c**. Elemental mappings (**Figures 2d–2h**) reveal that Co and O are homogeneously distributed in the selected areas, and the amorphous carbon is coated on the surface of Co_3O_4 crystals. Raman measurements (**Figure S6**) also suggest a structural transformation of Co-species, consistent with XRD and TEM results, under various annealing conditions.

OER performance and breakdown characteristics

To assess the OER catalytic activity, the as-synthesized catalysts on CPs were first investigated in 0.5 M H_2SO_4 solution (pH ≈ 0.3) with electrochemical measurements. The solution resistance caused by ohmic potential drop (iR) was corrected by the electrochemical impedance spectroscopy (EIS) plot at high frequencies (**Figure S7**). The OER activity was recorded by linear sweep voltammetry (LSV) at a scan rate of 5 mV/s after cyclic voltammetry scans for *ca.* 10 cycles when the electrode reached stability. As shown in supporting **Figure S8**, the OER overpotential at -10 mA/cm^2 for the Co_3O_4@C/CP catalyst decreases with deposition time of Co-species until 50 min, then increases afterwards. It indicates that the surface area of the catalysts increases with deposition time and hence their OER performance is enhanced. When the

electroplating time was extended to 60 min, the cross-sectional thickness of the Co_3O_4 sheet ensemble likely becomes too thick to allow efficient charge transport from electrolytes to the conducting CP substrate, and thus led to the performance decrease. For the two-step annealing process, we have also optimized the temperature of the first annealing step in vacuum (5 mTorr), and 350 ^oC is found to be optimal for OER performance (**Figure S9a**). The XRD patterns in supporting **Figure S9b** show that the decreased OER performance caused by a higher vacuum annealing temperature such as 600 ^oC and 900 ^oC is attributed to the transformation of Co-species to into unwanted metal Co and CoO.

Figure 3a compiles the polarization curves of different catalysts including CoO/CP, Co_3O_4@C/CP and the Co_3O_4/CP prepared with various annealing temperatures. For comparison, the Co_3O_4/CP and RuO_2/CP coated with a Nafion membrane are also included in the Figure, where the Nafion is commonly used as a capping layer to protect the catalysts from exfoliation during OER. The onset potentials of the electroplated catalysts Co_3O_4@C/CP, CoO/CP and Co_3O_4/CP with one-step and two-step treatments are all similar (*ca.* 1.54 V), where they achieve current densities of 10, 20, and 100 mA/cm^2 at overpotentials of 370, 390 and 460 mV, respectively. The overpotential at the current density of 10 mA/cm^2 is typically used for evaluating the electrochemical activity of an OER catalyst. Although the overpotential 370 mV for Co_3O_4@C/CP (at 10 mA/cm^2) is higher than the state-of-art Nafion-coated RuO_2/CP catalyst (220 mV), it is still lower than that of the Nafion-coated Co_3O_4/CP (420 mV) as well as that of Co_3O_4/Ti (about 450 mV) [46].

The electrocatalytic activity of a given material is normally proportional to its active surface area [53], which is strongly correlated to the capacitance of the double layer at the solid-liquid interface with cyclic voltammetry. To obtain the double layer capacitance, the potential is

scanned from 1.10 to 1.24 V at varying scan rates in a non-Faradaic potential window (see supporting **Figure S10**) and the resulted current density plotted against the scan rate at 1.17 V is shown in **Figure 3b**. The capacitance of Co_3O_4@C/CP is 113.3 mF/cm^2, which is *ca.* 3 times higher than that of Nafion-coated Co_3O_4 nanoparticles on CP (38.4 mF/cm^2) under the same catalyst loading amount. In this Figure, the capacitance for the acid-treated CP is also shown (25.0 mF/cm^2) as a reference. These results suggest that the electrochemically Co_3O_4 sheets possess a higher active surface area than Co_3O_4 nanoparticles on CP.

Figure 3c shows the Tafel plots for various OER catalysts of interest. The Tafel slope of Co_3O_4@C/CP catalyst is *ca.* 82 mV/dec (close to the Nafion-coated RuO_2/CP), which is much smaller than that of Nafion-coated Co_3O_4/CP (*ca.* 112 mV/dec) or CoO/CP (106 mV/dec). This suggests that the Co_3O_4@C/CP is an efficient catalyst for OER. In addition to the high OER efficiency in an acidic solution, this catalyst also presents superior activity in an alkaline solution, where we show the polarization curve and Tafel slope (68.8 mV/dec) for the Co_3O_4@C/CP in supporting **Figure S11**. It is observed that the overpotential to generate 10 mA/cm^2 is only 310 mV in 1.0 M KOH, which is lower than most of the reported non-precious alkaline OER electrocatalysts [54-56]. We note that the catalyst Co_3O_4/CP exhibits a lower Tafel slope 70 mV/dec compared to that of the Co_3O_4@C/CP. This is most likely due to carbon coating which retards the mass transport between the electrolyte and Co_3O_4 surface. However, the stability of Co_3O_4@C/CP is the highest among the OER catalysts developed in this work.

The electrochemical stability at a constant current density 100 mA/cm^2 is further studied and results are presented in **Figure 3d**. The actual electrode potential gradually increases with time for all investigated OER electrocatalysts. The potential sharply rises to 2.0 V after 8.8 h for CoO/CP (1h vacuum annealed), 56.4 h for Co_3O_4/CP (air annealed for 5h), 68.9 h for Co_3O_4/CP

(vacuum annealed for 1h + air annealed for 4h) and 86.8 h Co_3O_4@C/CP. The CoO/CP was the least stable one as expected due to its instability in the acidic pH. The Co_3O_4/CP prepared by the two-step process (vacuum 1h + air 4h) showed longer catalyst lifetime compared with that prepared by a one-step annealing (air 5h). Note that the conventional nafion-blended catalysts Co_3O_4@nafion/CP and RuO_2@nafion/CP do not exhibit good OER stability as shown in the figure 3d. In addition to the chemical stability of the catalysts, several factors have been identified as the causes for OER electrode failure. These included low conductivity of the catalysts and weak adhesion strength between catalysts and substrates [57]. The least OER stability found for the Co_3O_4/CP prepared by one-step annealing (air 5h) is attributed to a weak interface interaction between the catalyst and substrate, where the annealing in oxygen-rich environments would largely degrade the surface of the CP substrates. As shown in **Figure 3d**, the addition of vacuum annealing before oxidation in air considerably improved the OER stability of Co_3O_4. These observations indicate that the OER stability is not only determined by the chemical stability of the catalysts but also by the adhesion between Co_3O_4 and the substrate. For better understanding the important of interface adhesion, we have compared the OER stability for the catalysts grown on an ethanol-wetted CP and an acid-oxidized CP. All other experimental conditions are kept the same. As shown in **Figure S12**, the stability of Co_3O_4@C/CP (acid-oxidized) is better than the Co_3O_4@C/CP (ethanol-wetted). Note that the –OH and -COOH groups on CP produced by acid-treatment play the roles to bind to the Co_3O_4-catalysts. The result reveals that the interfacial bonding plays a key role in the stability of the catalysts. The coated carbon layers effectively avoided the direct degradation of CP surface as well as provided a mechanical supporting layer to further inhibit the exfoliation of the catalyst from the substrate. It is noteworthy pointing out that the electrochemically deposited catalysts

possess superior stability compared with those pre-calcined catalysts casted on substrates. This argument is corroborated by the fact that drop-casted Co_3O_4 on CP covered by Nafion shows a much shorter life time around 1.5 h as shown in **Figure 3d**. Note that the lifetime for the Nafion-coated RuO_2/CP, the best novel metal based OER catalysts, is around 46 h, which is still shorter than most of our Co_3O_4 catalysts on CP. In order to further illustrate the characteristics of our two-steps prepared catalysts, we also investigated the stability of the CoO/CP and Co_3O_4@C/CP catalysts in 1.0 M KOH solution as shown in supporting **Figure S11**. The lifetime (reaching potential 2.0 V at a constant current density of 100 mA/cm^2) is 292.7 h and 413.8 h, respectively. It is to be noted that the 100 mA/cm^2 is a relatively higher current density for breakdown test and most of literature works consider only 10 mA/cm^2 as the testing current density [58, 59]. **Table 1** compares our results and the available stability data from the literature, where we conclude that our proposed Co_3O_4 OER catalysts are superior in activity and lifetime.

Table 1. Comparison of catalytic performances and stability for a variety of OER catalysts.

Catalysts	substrate	η_{10} (mV)	Tafel slope (mV/dec)	Test condition	Stability (h)	Electrolyte
Co_3O_4@C	CP	370	82	100 mA/cm^2	86.8	0.5 M H_2SO_4
(this study)		310	69	100 mA/cm^2	413.8	1.0 M KOH
$Ir_{0.2}Ru_{0.8}O_2$[60]	Glassy carbon			50 mA/cm^2	>11	0.5 M H_2SO_4
PbO_2+RuO_2[61]	Au	251	~60	100 mA/cm^2	<55	0.5 M H_2SO_4
IrO_2[62]	Glassy carbon	330		~15 mA/cm^2	>4	0.5 M H_2SO_4
(Ir,Sn,Nb)O_2[63]	Ti foil			10 mA/cm^2	>44	1.0 M H_2SO_4
$IrNi_x/IrO_2$[40]	Sb-doped SnO_x			1 mA/cm^2	>20	0.05 M H_2SO_4
DNA@IrO_2[64]	Glassy carbon	312	32/90	~10.3 mA/cm^2	>12	0.1 M NaOH
Reduced Co_3O_4[65]	Glassy carbon	400	72	~9 mA/cm^2	>1.7	1.0 M KOH
Co_3O_4 NCs[66]	Carbon paper	320	101	10 mA/cm^2	>1	1.0 M KOH
CoP-MNA[67]	Nickel foam	290	65	10 mA/cm^2	>32	1.0 M KOH
Co_3O_4[68]	N-porous carbon	390	72	~20 mA/cm^2	>1.7	0.1 M KOH

Surface and interface structures

To further give support to the above arguments, Raman spectroscopy is used to probe into the integrity of the CP, in particular the interfacial area between CP and catalysts. The G-band at

~1585 cm^{-1} is associated with the sp^2 carbon atom vibrations [69], and the 2D band at ~2725 cm^{-1} is originated from a double resonance process: phonon-electron band structure [70]. The D-band peak of raw-CP at ~1370 cm^{-1} originate from the disordered structures in sp^2 hybridized carbon materials [71]. As shown in **Figure 4**, the ratio of I_D/I_G is 0.91 for the CP after annealing in air at 350 ^oC for 5 h, which is higher than the 0.62 for that annealed in vacuum (350 ^oC for 1 h). This suggests that the surface structure of CP is significantly degraded after calcination in air. Yet, vacuum annealing does not lead to our desired Co_3O_4 catalyst and hence the annealing in air is necessary. Interestingly, the two-step annealing process (1h vacuum + 4h in air) gives the ratio of I_D/I_G 0.60, indicating that the 1^{st} step treatment in vacuum is critical for stabilizing the CP surface structure. This is likely one of the reasons that Co_3O_4/CP prepared with the two-step annealing exhibits excellent OER stability as shown in **Figure 3d**.

To investigate the atomic composition and the chemical state of the as-prepared catalysts, we carried out X-ray photoelectron spectroscopy (XPS) measurements. As shown in supporting **Figure S13**, XPS spectra indicate that all the prepared samples contain C, O and Co elements with no other impurities. **Figure 5a** shows high resolution Co 2p spectrum of the sample obtained from Co_3O_4@C/CP, which consists of two main broad peaks at 779.6 and 794.7 eV corresponding to $2p_{3/2}$, $2p_{1/2}$ spin orbit lines respectively. The spectrum also contains weak satellite structures at the high binding energy side of $2p_{1/2}$ and $2p_{3/2}$ main peaks, which indicates the existence of Co oxide form [72, 73]. In order to identify the oxidation state of Co, peak fitting of Co $2p_{3/2}$ is conducted. The approach used for the peak fitting is similar to the one used by Biesinger *et al.* [74], ie, fitting of a broad main peak combined with the satellite structure. A Shirley background is applied across the Co $2p_{3/2}$ peak of the spectrum. The Co $2p_{3/2}$ from Co_3O_4@C/CP is well fitted using a combination of the parameters derived from both Co_3O_4 and

$Co(OH)_2$ standard samples [74, 75]. The results indicate that the sample contains 90.2% of Co_3O_4 and 9.8% of $Co(OH)_2$. Similar fitting parameters were used for Co_3O_4/CP (vacuum 1h + air 4h, **Figure 5b**) and Co_3O_4/CP (air 5h, **Figure 5c**). The composition of Co_3O_4/CP prepared by two-steps is 79.0% of Co_3O_4 and 21.0% of $Co(OH)_2$. The composition of Co_3O_4/CP (air 5h) is 84.0% of Co_3O_4 and 16.0% of $Co(OH)_2$. The Co $2p_{3/2}$ from CoO/CP (vacuum 1h, **Figure 5d**) is well fitted using a combination of the parameters derived from Co metallic, CoO and $Co(OH)_2$ standard samples [74]. The results indicate that the CoO/CP contains 8.8% of Co, 4.3% of $Co(OH)_2$ and 86.9% of CoO. The results analyzed above show that most of Co-species/CP will transform into CoO/CP under vacuum heating condition firstly, and it will further oxidize into Co_3O_4/CP with some $Co(OH)_2$/CP in air gas flow, which is similar with surface composition of the Co-species/CP calcined in air directly. However, they are greatly different from the carbon coated Co_3O_4/CP. The coated carbon could apparently reduce the content of $Co(OH)_2$/CP species. We like to add a note that XPS only provides the bonding information at the surfaces. We do not see obvious diffraction peaks of $Co(OH)_2$ from XRD. Therefore, we believe that the $Co(OH)_2$-species revealed in XPS are only on the Co_3O_4 surfaces, likely derived from the surface reaction of Co_3O_4 and the adsorbed thin moisture layers. Hence, the presence of surface $Co(OH)_2$ groups is not the dominating factor for the OER stability.

Conclusion

In this work, a facile strategy based on a thin protection carbon layer and two-step calcination methods is proposed to synthesize highly OER-stable catalysts in acid and alkaline solutions. The stability of synthesized Co_3O_4@C/CP is found to be better than the state-of-art RuO_2/CP at high current densities. The two-step calcination process apparently avoids the degradation of CP

surface and thus enhances the interfacial strength between catalysts and substrates, leading to high OER stability in acids. Moreover, a thin layer of carbon coating could effectively avoid the catalyst exfoliation from the substrate. The catalysts proposed in this study shows great promises for cheap and highly stable OER electrocatalysts, which can be integrated to PEM-based hydrolyzers for high-rate production of hydrogen.

Acknowledgements

This research was supported by KAUST and SABIC, Saudi Arabia.

References:

[1] D. Voiry, H. Yamaguchi, J. Li, R. Silva, D.C.B. Alves, T. Fujita, M. Chen, T. Asefa, V.B. Shenoy, G. Eda, M. Chhowalla, Nat. Mater. 12 (2013) 850-855.
[2] R. Subbaraman, D. Tripkovic, D. Strmcnik, K.-C. Chang, M. Uchimura, A.P. Paulikas, V. Stamenkovic, N.M. Markovic, Science 334 (2011) 1256-1260.
[3] J. Yang, D. Voiry, S.J. Ahn, D. Kang, A.Y. Kim, M. Chhowalla, H.S. Shin, Angew. Chem. Int. Ed. 52 (2013) 13751-13754.
[4] Z. Zeng, C. Tan, X. Huang, S. Mao, H. Zhang, Energy Environ. Sci. 7 (2014) 797-803.
[5] J. Miao, F.-X. Xiao, H.B. Yang, S.Y. Khoo, J. Chen, Z. Fan, Y.-Y. Hsu, H.M. Chen, H. Zhang, B. Liu, Sci. Adv. 1 (2015) e1500259.
[6] J. Chen, X.-J. Wu, L. Yin, B. Li, X. Hong, Z. Fan, B. Chen, C. Xue, H. Zhang, Angew. Chem. Int. Ed. 54 (2015) 1210-1214.
[7] C.-B. Ma, X. Qi, B. Chen, S. Bao, Z. Yin, X.-J. Wu, Z. Luo, J. Wei, H.-L. Zhang, H. Zhang, Nanoscale 6 (2014) 5624-5629.
[8] A.J. Smith, Y.-H. Chang, K. Raidongia, T.-Y. Chen, L.-J. Li, J. Huang, Adv. Energy Mater. 4 (2014) 1400398.
[9] Y.-H. Chang, C.-T. Lin, T.-Y. Chen, C.-L. Hsu, Y.-H. Lee, W. Zhang, K.-H. Wei, L.-J. Li, Adv. Mater. 25 (2013) 756-760.
[10] P. Jiang, Q. Liu, Y. Liang, J. Tian, A.M. Asiri, X. Sun, Angew. Chem. Int. Ed. 53 (2014) 12855-12859.
[11] Y.-H. Chang, F.-Y. Wu, T.-Y. Chen, C.-L. Hsu, C.-H. Chen, F. Wiryo, K.-H. Wei, C.-Y. Chiang, L.-J. Li, Small 10 (2014) 895-900.
[12] T.-Y. Chen, Y.-H. Chang, C.-L. Hsu, K.-H. Wei, C.-Y. Chiang, L.-J. Li, Int. J. Hydrogen Energy 38 (2013) 12302-12309.
[13] X. Yang, A.-Y. Lu, Y. Zhu, S. Min, M.N. Hedhili, Y. Han, K.-W. Huang, L.-J. Li, Nanoscale 7 (2015) 10974-10981.
[14] Q. Liu, J. Tian, W. Cui, P. Jiang, N. Cheng, A.M. Asiri, X. Sun, Angew. Chem. Int. Ed. 53 (2014) 6710-6714.
[15] X. Yang, A.-Y. Lu, Y. Zhu, M.N. Hedhili, S. Min, K.-W. Huang, Y. Han, L.-J. Li, Nano Energy 15 (2015) 634-641.
[16] Z. Yin, B. Chen, M. Bosman, X. Cao, J. Chen, B. Zheng, H. Zhang, Small 10 (2014) 3537-3543.
[17] Q. Lu, Y. Yu, Q. Ma, B. Chen, H. Zhang, Adv. Mater. 28 (2016) 1917-1933.
[18] S. Chen, J. Duan, M. Jaroniec, S.-Z. Qiao, Adv. Mater. 26 (2014) 2925-2930.

[19] W. Zhou, X.-J. Wu, X. Cao, X. Huang, C. Tan, J. Tian, H. Liu, J. Wang, H. Zhang, Energy Environ. Sci. 6 (2013) 2921-2924.
[20] K. Fominykh, P. Chernev, I. Zaharieva, J. Sicklinger, G. Stefanic, M. Döblinger, A. Müller, A. Pokharel, S. Böcklein, C. Scheu, T. Bein, D. Fattakhova-Rohlfing, ACS Nano 9 (2015) 5180-5188.
[21] W. Ma, R. Ma, C. Wang, J. Liang, X. Liu, K. Zhou, T. Sasaki, ACS Nano 9 (2015) 1977-1984.
[22] J. Nai, H. Yin, T. You, L. Zheng, J. Zhang, P. Wang, Z. Jin, Y. Tian, J. Liu, Z. Tang, L. Guo, Adv. Energy Mater. 5 (2015) 1401880.
[23] Y. Meng, W. Song, H. Huang, Z. Ren, S.-Y. Chen, S.L. Suib, J. Am. Chem. Soc. 136 (2014) 11452-11464.
[24] R. Liu, F. Liang, W. Zhou, Y. Yang, Z. Zhu, Nano Energy 12 (2015) 115-122.
[25] L.-A. Stern, l. feng, F. Song, X. Hu, Energy Environ. Sci. 8 (2015) 2347-2351.
[26] J. Ryu, N. Jung, J.H. Jang, H.-J. Kim, S.J. Yoo, ACS Catal. 5 (2015) 4066-4074.
[27] M. Ledendecker, S. Krick Calderón, C. Papp, H.-P. Steinrück, M. Antonietti, M. Shalom, Angew. Chem. Int. Ed. 54 (2015) 12361-12365.
[28] M.-R. Gao, X. Cao, Q. Gao, Y.-F. Xu, Y.-R. Zheng, J. Jiang, S.-H. Yu, ACS Nano 8 (2014) 3970-3978.
[29] T. Liu, Q. Liu, A.M. Asiri, Y. Luo, X. Sun, Chem. Commun. 51 (2015) 16683-16686.
[30] Y. Zhao, R. Nakamura, K. Kamiya, S. Nakanishi, K. Hashimoto, Nat. Commun. 4 (2013).
[31] M. Carmo, D.L. Fritz, J. Mergel, D. Stolten, Int. J. Hydrogen Energy 38 (2013) 4901-4934.
[32] Y. Lee, J. Suntivich, K.J. May, E.E. Perry, Y. Shao-Horn, J. Phys. Chem. Lett. 3 (2012) 399-404.
[33] M.E.G. Lyons, S. Floquet, Phys. Chem. Chem. Phys. 13 (2011) 5314-5335.
[34] N. Mamaca, E. Mayousse, S. Arrii-Clacens, T.W. Napporn, K. Servat, N. Guillet, K.B. Kokoh, Appl. Catal. B-Environ. 111–112 (2012) 376-380.
[35] T. Reier, Z. Pawolek, S. Cherevko, M. Bruns, T. Jones, D. Teschner, S. Selve, A. Bergmann, H.N. Nong, R. Schlögl, K.J.J. Mayrhofer, P. Strasser, J. Am. Chem. Soc. 137 (2015) 13031-13040.
[36] C. Wang, Y. Sui, G. Xiao, X. Yang, Y. Wei, G. Zou, B. Zou, J. Mater. Chem. A 3 (2015) 19669-19673.
[37] A. Shinde, R.R. Jones, D. Guevarra, S. Mitrovic, N. Becerra-Stasiewicz, J. Haber, J. Jin, J. Gregoire, Electrocatalysis 6 (2015) 229-236.
[38] G. Li, H. Yu, X. Wang, D. Yang, Y. Li, Z. Shao, B. Yi, J. Power Sources 249 (2014) 175-184.
[39] V.K. Puthiyapura, S. Pasupathi, S. Basu, X. Wu, H. Su, N. Varagunapandiyan, B. Pollet, K. Scott, Int. J. Hydrogen Energy 38 (2013) 8605-8616.
[40] H.N. Nong, H.-S. Oh, T. Reier, E. Willinger, M.-G. Willinger, V. Petkov, D. Teschner, P. Strasser, Angew. Chem. Int. Ed. 54 (2015) 2975-2979.
[41] R. Kötz, H. Neff, S. Stucki, J. Electrochem. Soc. 131 (1984) 72-77.
[42] R. Kötz, H.J. Lewerenz, P. Brüesch, S. Stucki, J. Electroanal. Chem. Interfacial Electrochem. 150 (1983) 209-216.
[43] Z. Zhuang, W. Sheng, Y. Yan, Adv. Mater. 26 (2014) 3950-3955.
[44] Y. Liang, Y. Li, H. Wang, J. Zhou, J. Wang, T. Regier, H. Dai, Nat. Mater. 10 (2011) 780-786.
[45] G.A. Kozhina, A.N. Ermakov, V.B. Fetisov, A.V. Fetisov, K.Y. Shunyaev, Russ. J. Electrochem. 45 (2009) 1170-1175.
[46] L.M. Da Silva, J.F.C. Boodts, L.A. De Faria, Electrochim. Acta 46 (2001) 1369-1375.
[47] M. Bernicke, E. Ortel, T. Reier, A. Bergmann, J. Ferreira de Araujo, P. Strasser, R. Kraehnert, ChemSusChem 8 (2015) 1908-1915.
[48] K.S. Kadakia, P.H. Jampani, O.I. Velikokhatnyi, M.K. Datta, S.K. Park, D.H. Hong, S.J. Chung, P.N. Kumta, J. Power Sources 269 (2014) 855-865.
[49] A.A. El-Moneim, N. Kumagai, K. Asami, K. Hashimoto, Mater. Trans. 46 (2005) 309-316.
[50] L.-F. Chen, Z.-Y. Yu, X. Ma, Z.-Y. Li, S.-H. Yu, Nano Energy 9 (2014) 345-354.
[51] W. Guo, C. Xu, X. Wang, S. Wang, C. Pan, C. Lin, Z.L. Wang, J. Am. Chem. Soc. 134 (2012) 4437-4441.
[52] L. Zhengquan, G. Huichen, Q. Haisheng, H. Yong, Nanotechnology 21 (2010) 315105.
[53] S.K. Singh, V.M. Dhavale, S. Kurungot, ACS Appl. Mater. Interfaces 7 (2015) 442-451.
[54] F. Song, X. Hu, J. Am. Chem. Soc. 136 (2014) 16481-16484.
[55] S. Mao, Z. Wen, T. Huang, Y. Hou, J. Chen, Energy Environ. Sci. 7 (2014) 609-616.
[56] Y. Yang, H. Fei, G. Ruan, J.M. Tour, Adv. Mater. 27 (2015) 3175-3180.
[57] G. Chen, X. Chen, P.L. Yue, J. Phys. Chem. B 106 (2002) 4364-4369.
[58] Y. Zhu, W. Zhou, Y. Chen, J. Yu, M. Liu, Z. Shao, Adv. Mater. 27 (2015) 7150-7155.
[59] L. Wu, Q. Li, C.H. Wu, H. Zhu, A. Mendoza-Garcia, B. Shen, J. Guo, S. Sun, J. Am. Chem. Soc. 137 (2015) 7071-7074.
[60] J. Cheng, H. Zhang, G. Chen, Y. Zhang, Electrochim. Acta 54 (2009) 6250-6256.

[61] M. Musiani, F. Furlanetto, R. Bertoncello, J. Electroanal. Chem. 465 (1999) 160-167.
[62] W. Hu, Y. Wang, X. Hu, Y. Zhou, S. Chen, J. Mater. Chem. 22 (2012) 6010-6016.
[63] K. Kadakia, M.K. Datta, O.I. Velikokhatnyi, P. Jampani, S.K. Park, P. Saha, J.A. Poston, A. Manivannan, P.N. Kumta, Int. J. Hydrogen Energy 37 (2012) 3001-3013.
[64] S. Anantharaj, E.K. Pitchiah, S. Kundu, J. Mater. Chem. A 3 (2015) 24463-24478.
[65] Y. Wang, T. Zhou, K. Jiang, P. Da, Z. Peng, J. Tang, B. Kong, W.-B. Cai, Z. Yang, G. Zheng, Adv. Energy Mater. 4 (2014) 1400696.
[66] S. Du, Z. Ren, J. Zhang, J. Wu, W. Xi, J. Zhu, H. Fu, Chem. Commun. 51 (2015) 8066-8069.
[67] Y.-P. Zhu, Y.-P. Liu, T.-Z. Ren, Z.-Y. Yuan, Adv. Funct. Mater. 25 (2015) 7337-7347.
[68] Y. Hou, J. Li, Z. Wen, S. Cui, C. Yuan, J. Chen, Nano Energy 12 (2015) 1-8.
[69] S.-X. Guo, Y. Liu, A.M. Bond, J. Zhang, P. Esakki Karthik, I. Maheshwaran, S. Senthil Kumar, K.L.N. Phani, Phys. Chem. Chem. Phys. 16 (2014) 19035-19045.
[70] M. Hiramatsu, H. Kondo, M. Hori, Graphene Nanowalls, 2013.
[71] G. Sun, J. Liu, X. Zhang, X. Wang, H. Li, Y. Yu, W. Huang, H. Zhang, P. Chen, Angew. Chem. Int. Ed. 53 (2014) 12576-12580.
[72] D. Li, X. Liu, Q. Zhang, Y. Wang, H. Wan, Catal. Lett. 127 (2009) 377-385.
[73] A. Younis, D.W. Chu, X. Lin, J. Lee, S. Li, Nanoscale Res. Lett. 8 (2013) 36.
[74] M.C. Biesinger, B.P. Payne, A.P. Grosvenor, L.W.M. Lau, A.R. Gerson, R.S.C. Smart, Appl. Surf. Sci. 257 (2011) 2717-2730.
[75] R. Madhu, V. Veeramani, S.-M. Chen, A. Manikandan, A.-Y. Lo, Y.-L. Chueh, ACS Appl. Mater. Interfaces 7 (2015) 15812-15820.

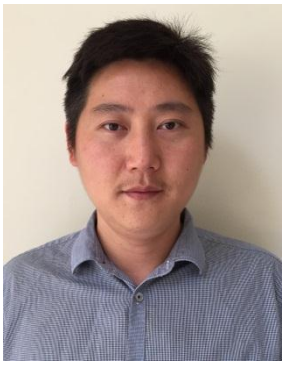

Dr. Xiulin Yang received his PhD degree in Institute of Chemistry, Chinese Academy of Science in 2013. Currently, he is a postdoc in Prof. Dr. Lain-Jong (Lance) Li group at King Abdullah University of Science and Technology, Saudi Arabia. His research interest focuses on design and application of various nanomaterials for water splitting, fuel cells, water treatment and gas separation.

Henan Li received her Bachelor's degree (BE) in Materials Science and Engineering from Nanyang Technological University in 2008. She obtained her PhD in 2014 at the same department supported by Nanyang President's Graduate Scholarship. She is currently working as a postdoctoral research fellow at KAUST and her research is focused on characterizations of 2-dimensional materials and their energy applications.

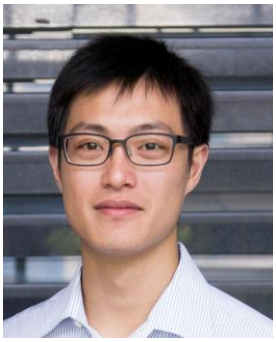

Mr. Ang-Yu Lu received his BSc and MSc in Engineering and System Science at National Tsing Hua University, Taiwan. Since 2010, he was a research assistant in at Academia Sinica for 4 years. Currently, he is a technical specialist in 2D Material Lab at KAUST, Saudi Arabia. His research interests in chemical vapor deposition synthesis and characterization of 2D materials and electrochemistry of water splitting.

Dr. Shixiong Min received his PhD in Physical Chemistry from Lanzhou Institute of Chemical Physics, Chinese Academic of Sciences, China, in 2013. He is an associate professor at Beifang University of Nationalities, China. He has a postdoctoral fellow in KAUST Catalysis Research Center, King Abdullah University of Science and Technology, working with Professor Kuo-Wei Huang and Lain-Jong Li since March, 2014. His research interests include transition-metal-based complexes and metal catalysts for electrocatalytic reduction of carbon dioxide, advanced catalyst materials for water splitting reaction (HER and OER), semiconductor-based photocatalysts for the hydrogen production, carbon nanomaterial-based dye-sensitized photocatalytic systems for water reduction.

Zacharie Idriss is currently an undergraduate student in Electrical Engineering at Pennsylvania State University (USA). Before his tertiary education, he obtained his International Baccalaureate degree at the American International School in Riyadh. He received the US President's Education Awards Program for Outstanding Academic Achievement in 2013.

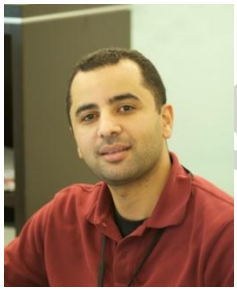

Dr. Mohamed Nejib Hedhili received his PhD in physics from University Pierre et Marie Curie, Paris VI, France in 1998. He was a postdoctoral research associate from 1998 to 1999 in the Laboratory for Surface Modification at the Rutgers University. He joined the faculty of physics as an assistant professor in 1999 at University of Tunis. In 2009, he took a Senior Research Scientist Position at KAUST. Since 2014, he has been working as the Team Lead of the Surface Analysis in the Imaging and Characterization

Laboratory of KAUST. His research interests include X-ray photoelectron spectroscopy of micro and nanomaterials.

Dr. Kuo-Wei Huang obtained his B.S. from National Taiwan University as a Dr. Yuan T. Lee Fellow, and Ph.D. from Stanford University as a Regina Casper Fellow. He is currently SABIC Chair Associate Professor in the Physical Sciences and Engineering Division at King Abdullah University of Science and Technology and the KAUST Catalysis Center. Prior to joining KAUST, he was Assistant Professor in National University of Singapore and a Gertrude and Maurice Goldhaber Distinguished Fellow at Brookhaven National Laboratory, where he still maintains solid collaborations. His research interests include renewable energy and synthetic and mechanistic studies of small molecule activation.

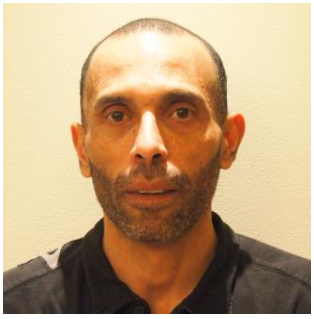

Hicham Idriss is Fellow at SABIC Corporate Research & Development (CRD) at KAUST, Saudi Arabia and Professor (Hon.), Department of Chemistry, University College London, UK.

He received his undergraduate and postgraduate education from the University of Strasbourg (France). Prior to joining SABIC he was Aberdeen Energy Futures Chair and Professor of Chemistry at the University of Aberdeen (UK). His main research work is on the surface reactions of metal oxides both at the experimental and computational levels. In the last decade, he has been focusing his research on hydrogen production from renewables both by thermal and photocatalytic methods. He has about 200 papers and over 50 patents/patents applications. He is member of the editorial board of Catalysis, Structure and Reactivity; Applied Catalysis B: Environmental; Catalysis Surveys from Asia; and the regional editor of Current Organocatalysis.

Dr. Lain-Jong (Lance) Li received BSc at National Taiwan University as a Dr. Yuan T. Lee Fellow and obtained MSc at the same department. After 5 years of R&D at the TSMC, he obtained PhD in condensed matter physics from Oxford University in 2006 as a Swire Scholarship Fellow. He was an assistant professor in MSE at Nanyang Tech. Univ. Singapore (2006-2009). Since 2010, he has become an Associate research fellow at Academia Sinica Taiwan. He started his Associate Professorship at KAUST, in 2014. His research interests include chemical vapor deposition and characterizations of 2-dimensional materials and their energy applications.

Figures

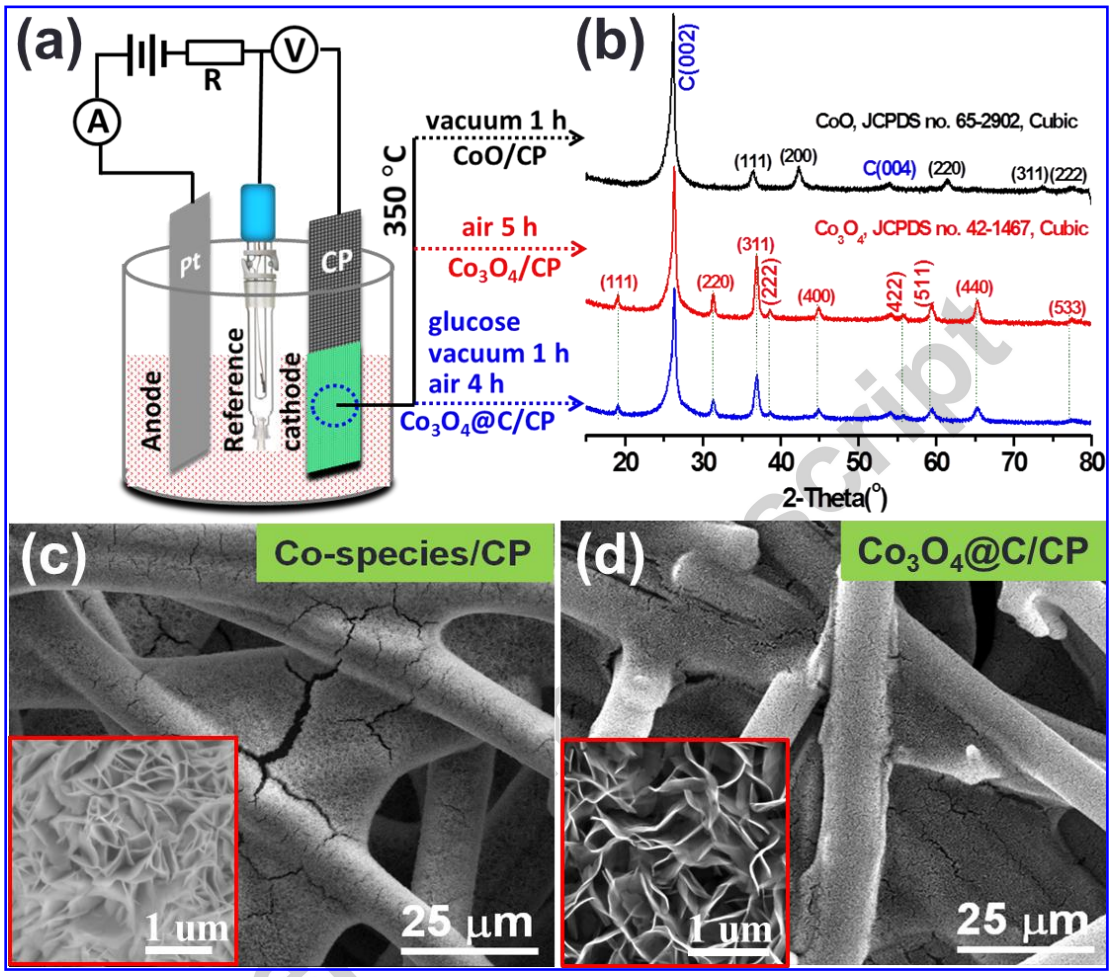

Figure 1. (a) Schematic diagram for the electroplating of Co-species on CP, where the subsequent treatment conditions are also indicated. (b) XRD patterns of the electrodes treated with various conditions indicated as CoO, Co_3O_4 and Co_3O_4@C respectively. SEM images of (c) electrodeposited Co-species on CP, and (d) the optimized electrode Co_3O_4@C/CP.

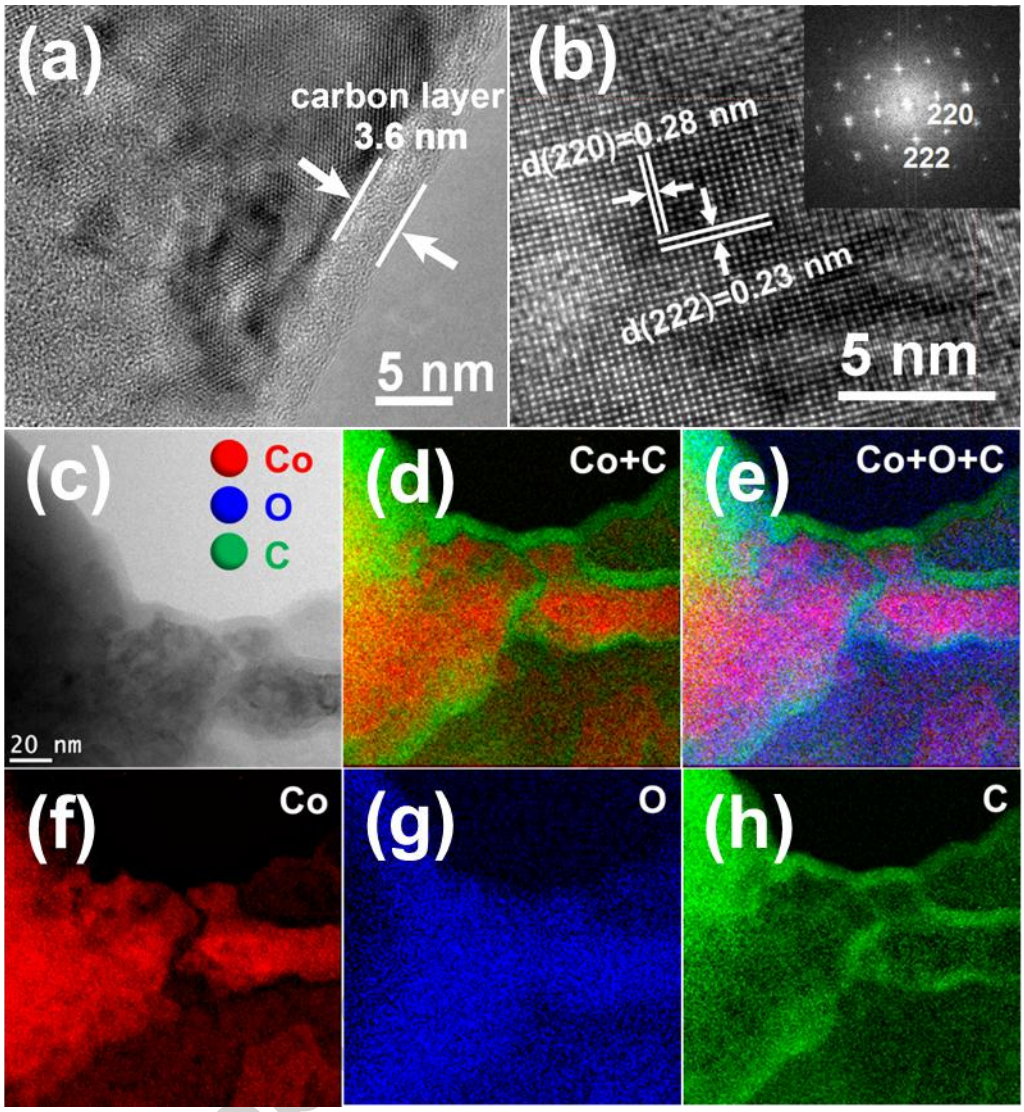

Figure 2. (a) TEM image and (b) high-resolution TEM image of the flake peeled off from the electrode Co_3O_4@C/CP. Inset b is the diffraction pattern. (c) HAADF-STEM image of Co_3O_4@C. (d, e) The reconstructed mappings with (d) Co and C, and (e) Co, C, and O based on the elemental mapping of the image field figure 2c for (f) Co in red color, (g) O in blur color, and (h) C in green color.

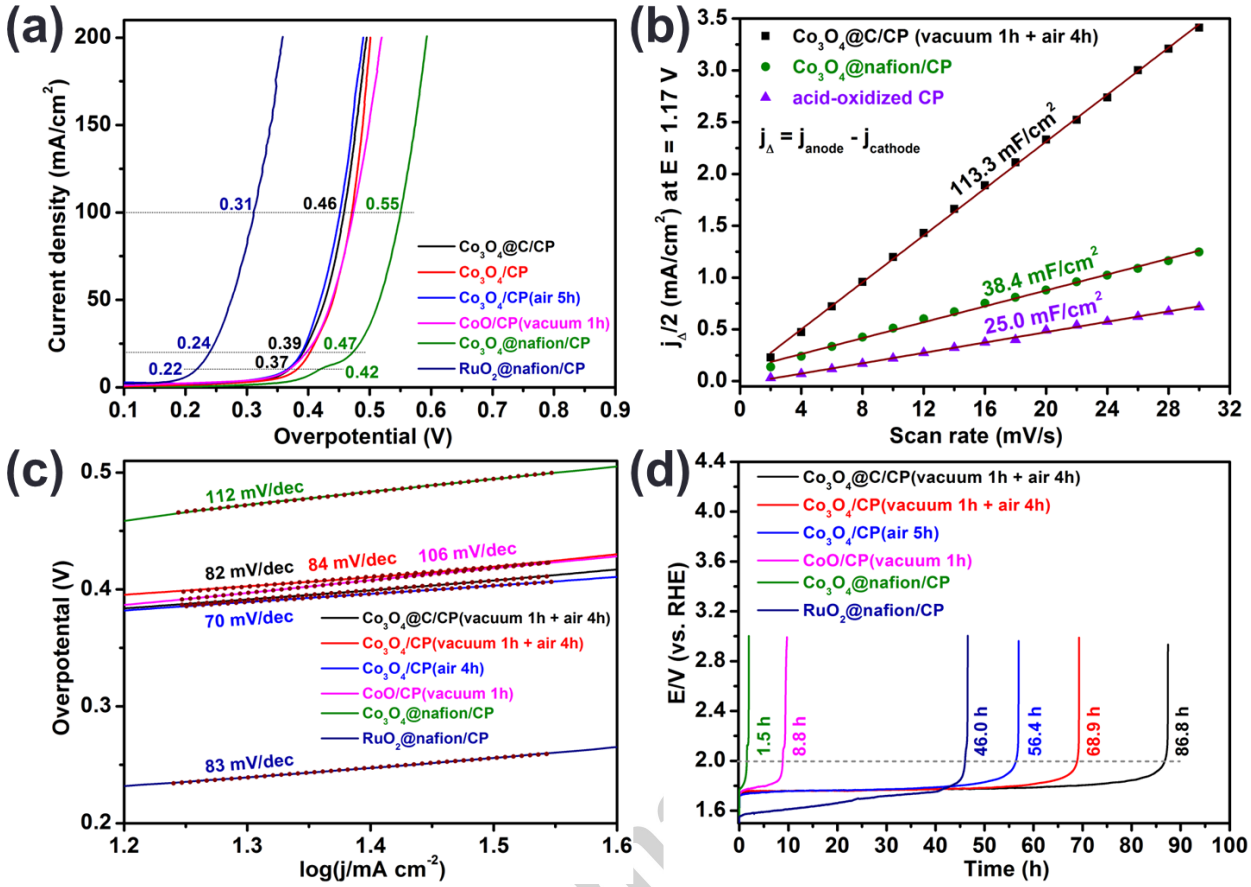

Figure 3. (a) Polarization curves of the Co_3O_4 and RuO_2 on CP catalysts synthesized by different methods measured in 0.5 M H_2SO_4 with a scan rate of 5 mV/s, where the current is normalized by the geometrical area of carbon fiber paper and the potential is after internal resistance correction; (b) Double-layer capacitance (C_{dl}) for the Co_3O_4@C/CP, Co_3O_4@nafion/CP and acid-oxidized CP; (c) Tafel slopes extracted from the polarization curves in (a); (d) Galvanostatic measurement at a current density of 100 mA/cm^2 for different electrocatalysts.

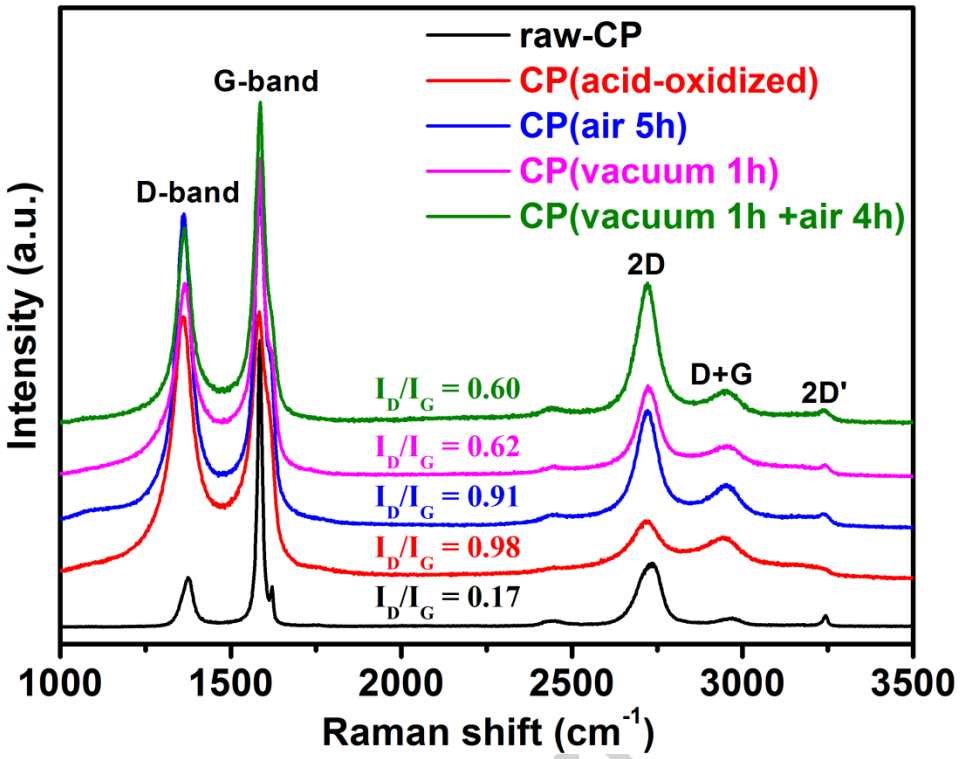

Figure 4. Raman spectrum of the raw-CP, acid-oxidized CP, acid-oxidized CP calcined in air 1 h, vacuum 1 h and two-steps heating at 350 ^{o}C, respectively.

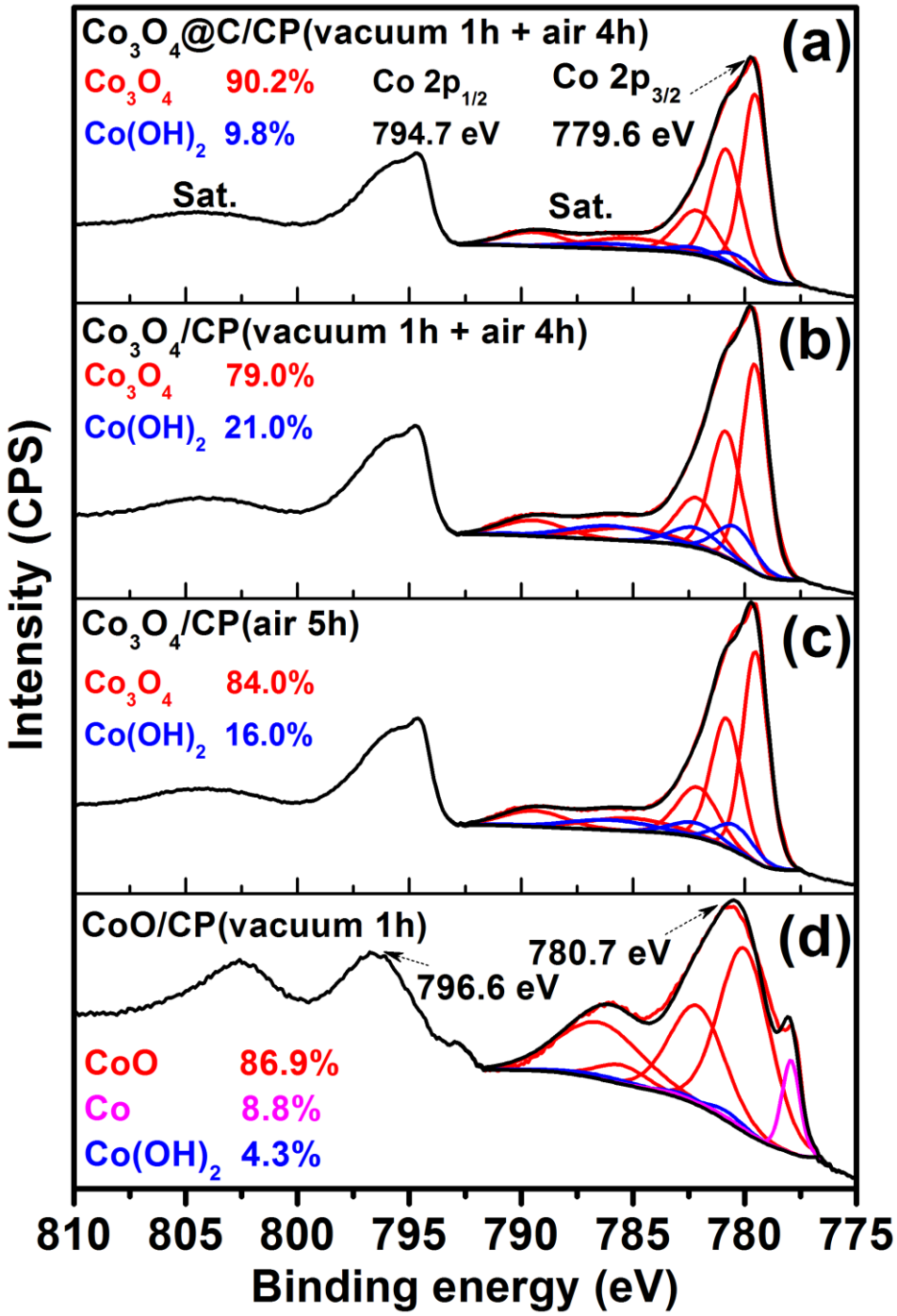

Figure 5. High-resolution XPS spectrum of Co 2p for (a) Co_3O_4@C/CP and (b) Co_3O_4/CP prepared by two-steps methods, (c) Co_3O_4/CP (air 5h) and (d) CoO/CP (vacuum 1h).

Highlights

- Carbon coated Co_3O_4 arrays on carbon fiber paper is obtained by electroplating methods combined two-step calcined treatments.
- The Co_3O_4@C/CP catalyst exhibits long-time stability at 100 mA/cm^2 for 86.8 h, and a small overpotential (370 mV) to reach 10 mA/cm^2 in 0.5 M H_2SO_4.
- The excellent stability is proved to be related with the carbon layer protection and the interface force between the catalysts and the substrate.

Graphical Abstract:

Carbon coated Co_3O_4 array on carbon fiber paper (Co_3O_4@C/CP) are developed by electroplating methods combined two-step calcined treatments. The prepared catalysts reveal highly efficient oxygen evolution reaction in 0.5 M H_2SO_4 with a small overpotential (370 mV) to reach 10 mA/cm^2, and long-time stability at 100 mA/cm^2 for 86.8 h. The excellent performance is proved to be related with the carbon layer protection and the interface force between the catalysts and the substrate.